

# CELL SWITCHES MODEL APPLYING MARKOV CHAIN STOCHASTIC MODEL CHECK ON BETWEEN TWO POPULATION WITH REGARDS TO MRNA AND PROTEINS AND NEURONS BOTH CLASSICALLY AND QUANTUM COMPUTATIONALLY

Qin He, Rubin Wang and Xiaochuan Pan

East China University of Science and Technology, Meilong 130, China

## ABSTRACT

*Arc, one virus-like gene, crucial for learning and memory, was discovered by researchers in neurological disorders fields, Arc mRNA's single directed path and allowing protein binding regional restrictively is a potential investigation on helping shuttle toxic proteins responsible for some diseases related to memory deficiency. Mean time to switching (MTS) is calculated explicitly quantifying the switching process in statistical methods combining Hamiltonian Markov Chain(HMC). The model derived from predator and prey with typeII functional response studies the mechanism of normals with intrinsic rate of increase and the persists with the instantaneous discovery rate and converting coefficients. During solving the results, since the numeric method is applied for the 2D approximation of Hamiltonion with intrinsic noise induced switching combining geometric minimum action method. In the application of Hamiltonian Markov Chain, the behavior of the conversion (between mRNA and proteins through 6 states from off to on ) is described with probabilistic conditional logic formula and the final concentration is computed with both Continuous and Discret Time Markov Chain(CTMC/DTMC) through Embedding and Switching Diffusion. The MTS, trajectories and Hamiltonian dynamics demonstrate the practical and robust advantages of our model on interpreting the switching process of genes (IGFs, Hax Arcs and etc.) with respects to memory deficiency in aging process which can be useful in further drug efficiency test and disease curing. Coincidentally, the Hamiltonian is also well used in describing quantum mechanics and convenient for computation with time and position information using quantum bits while in the second model we construct, switching between excitatory and inhibitory neurons, similarity of qubit and neuron is an interesting object as well. Especially with the interactions operated with phase gates, the excitation from the ground state to excitation state is a well analogue to the neuron excitation. Not only on theoretical aspect, the experimental methods in neuron switching model is also inspiring to quantum computing. Most basic one is as stimulate hippocampus can be identical to spontaneous neural excitation( $|g\rangle|e\rangle$ ), pi-pulse is utilized to drive the ground state to the higher state. There thus exists prosperous potential to study the transfer between states with our switch models both classical and quantum computationally.*

## KEYWORDS

*switching model, mean time to switching, Hamiltonian Markov Chain, geometric minimum action method, firing rate, neuron models, Hopfield network, excitation and inhibition, quantum computation, fast gates, phase estimation, sweep entanglement.*

## 1. INTRODUCTION

In cell biology, non-equilibrium stochastic process is of interest since the observation of experimental results are becoming of higher resolution, studying the molecules both with imaging and expression data are often conducted in both single and population (thousand) order, which basically described in stochastic process whether on a discrete or continuous scale with status changes either genotypically or phenotypically. Many problems are thus studied related to status switching, including cell regulatory networks, signal response on excitability and inhibition [1], (convinced by translational and transcriptional burst of expression for instances.), metastability among populations, (binding of ligands and proteins, forming of polymerases and etc.). In this paper, we first focus on the interaction among genes, mRNA, proteins and etc. To be more specific, while the switching problem among molecules can be studied on geno-type, including sequencing for single RNA, alignments and binding considering condons and etc, we stay on the switching with expression (concentration) only, which is simplified as modified population problem using Lotka-Volterra equations[3] of two populations only. Thus, rather than the competitor model (for instances, cell bifurcations.), we applied simulation of switching on predator model. The model is based on the following basic assumptions: Prey population (promoters) is fed with enough food all the time while the predator population of the predator (the persisters) depends on the size of prey (promoters).

To be more specific, while the switching problem among molecules can be studied on geno-type, including sequencing for single RNA, alignments and binding considering condons and etc, we stay on the switching with expression (concentration) only, which is simplified as modified population problem using Lotka-Volterra equations[3] of two populations only. Thus, rather than the competitor model (for instances, cell bifurcations.), we applied simulation of switching on predator model. The model is based on the following basic assumptions: Prey population (promoters) is fed with enough food all the time while the predator population of the predator (the persisters) depends on the size of prey(promoters).

In the next part, we focus on the interpretation of the working memory modelled through neuron interactions. Due to the slow oscillation, there occurs the up-state and down-state [4]. The solution to the differential equation is initialized on the two formula with regards to intrinsic oscillation  $dS/st$  and evolution of phase  $d\phi/dt$  respectively. The reduce to the normal form is completed with combination of firing model and leakage-gate model [5]. The parameters are solved analytically first and numerically simulated with experiment data.

In practical, for the first model. we mainly study the interaction of DNA and its interaction with the associated proteins.(Clinical data of Hax1 and HS1 is downloaded from Ensembl gene database[2]). On one hand, the switching model is calculated under the large deviation theory (LDT) [5] combining the least actions. The Markov chain[6] consider the states of the 2D coordinates (x; y) of mRNA numbers and protein numbers referencing the distribution of x, which follows the order  $O(1)$  while PX follows the time scale on  $O(1/e)$  and guaranteeing the variant of LDT hold with the transform of the expressions in single population. Only considering the process of diffusion case, we study the binding of hax1 with simple switching between on and off status under its interaction with HS1 seen as in the constant environment, i.e. the closed system at mean field. The dimer which can be cancelled out connect the binding between two single population. On the other hand, one numeric method is applied to solve the problem, making compare with the stochastic process[7] on ap-approximation equation of the mean switching time(MST) with the transform between two status (we studied the switching time with four situations, both multiplicative and asymptotic of single population and the binding and degradation between two population.) Again, this method is also calculated based on the Hamiltonians. We give out the MST with respect to  $N/N_c$  denoting N as the population number

of interest and  $N_c$  as the threshold of certain status (either of that population or the other population). Since our study only based on data in the process of transforming in the constant environment, extinction is not considered in this paper.

On contrary, the second model applies the deterministic model with the single unit model based on normal equation reduced after frequency transfer with firing rate model and leakage model on the relation between  $I$  and  $V$ . Similar as the first model, eigenvalues are solved with Jacobian matrix at the fixed stable point. This part gives the core algorithm as well. It represents the populations of NMDA, AMPA, GABA cells, separating the system into interacting networks [8]: Positive Network Task (PNT) and Negative Network Task (NNT). In PNT, the excitatory population AMPA and inhibitory population GABA interacted mutually while in NNT, the excitatory population NMDA interacts with inhibitory GABA. The connection in each population and each unit are all assumed to be bidirection with the weight difference only across populations. Similarly, the weight cross units are also different as neuron cannot connect from inhibitory population to excitatory population across unit, the weight accordingly can be seen as zero. And the global feedback of inhibitory network is thus constructed [9]. And in aim of exploring the transfer between states from another aspect, quantum computation is introduced as well. From the Hamiltonian as well, the interactions are studied on energy/power spectrum level clearly with not only related to time but also to the dynamics comprehensively. Due to comparison with classical switch model, we focus on the internal interactions as well. Thus, the switching phase analysis between ground state  $|g\rangle$  and higher state  $|e\rangle$  or Stark eigenstate  $|r\rangle$  were introduced. In the illustration of entanglement, the sweep operation [10] is chosen as its advantage of flexible and competitive. The fixed point finding in classical computation is adopted into the eigenstate define in quantum computation and here is exhibited with detail as well. More operation and demonstration with regards to Bell states/ GHZ [11] is also interesting although not the focus in this paper.

To study both intrinsic and extrinsic noise with the exciting and inhibiting bursts is the potential topic in the future. In the following contents, the first chapter is the proposition of the model, based on least action with LDT and MTS approximation with one stochastic differential equation (SDE) [13] separately; And the second chapter gives numeric experiments based on Hamilton Markov Chain[14] computation of the expression data of *hax1* and *HS1*; In the last chapter, the model is described in the normal logic formula with both probabilistic condition model[15] and the results are analysed with both Hamiltonian, realization size, convergence, the rewards computation taking the CTMC as Poisson process[15] and the reachability computation with the transfer kernel of switching diffusion[16] through DTMC. In the appendix, there also includes the complete proof of model with action  $S$  based on Hamilton not only based on the explicit equation in this paper. Some descriptive statistics and pre-computation based on the data can be accessed through link in availability. As the process related to motor coordination and function, the Hax's function in regulation, B cell's signal transduction can be further studied with more data considering its excitability and metastability functions with stimulation of drugs for instance in the future as well. And one computation applying DTMC with linear regression on previous work is made as the further extension of the model.

On one hand, as transformation on spectrum is of same computation scale level, for instance, the FFT on exponential computation, the base of normal and poisson distribution, it is natural as well to find some similar results in quantum computation. On the other hand, the property of neurons and qubits are similar, for instance all vs none (AVN) [17] and the network being heretic and some researches with regards to empiric model, either stochastically or deterministically, it is natural and beneficial to conduct research combing classical and quantomechanical computation and modelling.

## 2. PROPOSED MODEL

Molecular interactions are studied on phenotypic data of the mRNA and its associated protein, especially the trajectory of the production of hax1 and HS1 with interaction with each other through least action method combining diffusion process[18] in the first part while adopted model with neurons,... in the second in this paper. Furthermore, in solving the equation, one stochastic differentiation equation approximates the analytic solution and calculation of MST[19] based on converging with Hamiltonian quantities, finding three convergence points through eigenvalue of position quantities as well as satisfying  $H = 0$  and  $Hq = 0$  where  $q(P, X; PY)$  are momentum quantities. In the 3rd subsection, the transition is illustrated with belief graph first and then convert ratio are utilized in computing the discrete embedding of the continuous temporal logic. As comparison, the third subsection compute the discretized time markov chain as the approximation considering it as a hybrid systems.

### 2.1. Switching Model with Least Action

#### a. population defined as mRNA and proteins

First of all, we consider the dynamics of population of the interaction involved systems as diffusion[18], and thus the Hamiltonian  $H(x, \theta)$  is computed with the minimization of action (quasi-potential)[20] instead of some other methods, for instance WKB[14]. With the Lagrangian denoted with respect to Hamiltonian according to LDT:

$$L(x, y) = \sup_{\theta \in R_n} (\langle y, \theta \rangle - H(x, \theta)) = \langle y, \theta(x, y) \rangle - H(x, \theta(x, y))$$

Due to the maximizer  $\theta(x, y)$  being implicitly defined by  $H_\theta(x, \theta(x, y)) = y$ , we calculate the action from quasi-potential:

$$V(x_1, x_2) = \inf_{\tau > 0} \inf_{\psi \in C_{x_1}^{x_2}(0, \tau)} ST(\psi) = \inf_{\tau > 0} \inf_{\varphi \in C_{x_1}^{x_2}(0, 1)} \inf_{\psi \in C_{x_1}^{x_2}(0, \tau)} ST(\psi) = \inf_{\varphi \in C_{x_1}^{x_2}(0, 1)} S(\varphi)$$

So that for any  $\varphi \in C(0, 1)$  the action  $S(\varphi)$  is given by the equivalent four formula:

$$\begin{aligned} S(\varphi) &= \inf_{\tau > 0} \inf_{\psi \in C_{x_1}^{x_2}(0, \tau)} ST(\psi) \\ S(\varphi) &= \sup_{\theta: [0, 1] \rightarrow H(\varphi, \theta) = 0} \int_0^1 \langle \varphi', \theta(\varphi, \varphi') \rangle d\alpha \\ S(\varphi) &= \int_0^1 \langle \varphi', \theta(\varphi, \varphi') \rangle d\alpha \\ S(\varphi) &= d\alpha, \lambda = \lambda(\varphi, \varphi') \end{aligned}$$

Note that  $L(x, y)$  is the Lagrangian associated with the Hamiltonian  $H(x, \theta)$  with function  $\theta(x, y)$  and  $\lambda(x, y)$  are implicitly defined for all  $x \in D$  and  $y \in R^n \setminus \{0\}$  as the unique solution (solution  $(\theta, \lambda) \in R^n \times [0, \infty)$  of the system possessing zero value when  $\varphi = 0$  or  $\lambda(\varphi, \varphi') = 0$  setting the integrands to zero with:  $H(x, \theta) = 0, H_\theta(x, \theta) = \lambda y \leq \lambda$  where the lower bounds for  $S(\varphi)$  is directly achieved:

$$S(\varphi) = \inf_{\tau > 0} \inf_{\psi \in C_{x_1}^{x_2}(0, \tau)} S_\tau(\psi) \geq \int_0^1 \sup_{\theta: [0, 1] \rightarrow H(\varphi, \theta) = 0} \langle \varphi', \theta \rangle d\alpha \geq \int_0^1 \langle \varphi', \theta(\varphi, \varphi') \rangle d\alpha$$

utilizing the first equation of the four. Furthermore,  $S(\varphi)$ 's upper bound can also be obtained through defining a minimizing sequences  $(T_k, \psi_k), k \in \mathbb{N}$  with the following rescaling process: For every  $k \in \mathbb{N}$  let:  $\lambda_k(\alpha) = \max(\lambda(\varphi(\alpha), \varphi'(\alpha)), 1/k), \alpha \in [0, 1], B_k(\alpha) = d\alpha, \alpha \in [0, 1], T_k(\alpha) = B_k(1), B_k(t) = \varphi(B_k^{-1}(t)), t \in [0, T_k]$  Specifically, the inverse of  $B_k$  is approximated with the Brownian standard  $\sigma_x$  satisfying the  $\alpha_0(t) = \lambda_k(\alpha(t))$  and thus  $1/k \leq \alpha'(t) \leq |\lambda_k| \inf \leq \inf$  holds for all  $t \in [0, T_k]$  with the absolute continuity of  $\alpha(t)$ . And thus, the  $\psi_k$  is continuous in the whole

time sequence  $(0, T_k)$ , enabling the inverse process:  $t = t(\alpha) = G_k(\alpha)$  with  $dt = d\alpha/\lambda_k$  and  $\varphi'(\alpha) = \psi'(t)G'_k(\alpha) = \psi'(t)/\lambda_k(\alpha)$ .

$$\text{Thus, } S_T(\psi) = \int_0^{T_k} L(\varphi, \varphi \lambda'_k) / \lambda_k d\alpha$$

leading to the upper bound switching the integrate and limitation with  $k \rightarrow \inf$ , and with the proof in appendix B (in another work with landscape model) fulfilling the first order and second order conditions:  $\varphi' = H(\varphi, \theta)/\lambda$  is negative definite during the  $\theta$  maximizing process:  $L(\varphi, \lambda\varphi)/\lambda = \sup_{\theta \in \mathbb{R}^n} \langle \varphi', \theta \rangle - H(\varphi, \theta)/\lambda$  and guaranteeing them both fulfilled by  $\theta = \theta(\varphi, \varphi')$  with the second equation, so that upper bound here is the same as the integrands of the lower bound as well as holds the  $\theta = 0$  when the  $\lambda = 0$  is satisfied, and therefore:

$$\frac{L(\varphi, \varphi \lambda'_k)}{\lambda} = \langle \varphi', \theta \rangle - \frac{H(\varphi, \theta)}{\lambda} = \langle \varphi_0, \theta \rangle,$$

$$\theta = \theta(\varphi, \varphi')$$

The calculation can be found completely in Appendix B.

## b. population defined as exhibitory and inhibitory neurons

Similarly, the switching model combining two phenomenological models with regards to the membrane potential  $S_i$  for each cell  $i$  and the intrinsic oscillation characterized by phase  $\varphi_i$  is constructed (in each single unit, either positive network or negative network is formed by the transition between pyramidal neurons and interneurons [21]):

Initial from the resting state, the periodic motion consists of the intrinsic oscillation  $dS/dt$  with regards to  $\cos \varphi_i$  of the membrane potential  $S_i$  and the evolution of the phase  $d\varphi/dt$ , depending on the depolarization level:

$$\begin{cases} \frac{dS_i}{dt} = -S_i + \sum_{j=1}^N W_{ij} R(S_j) + C(\varphi_i) + I_i \\ \frac{d\varphi_i}{dt} = -w + (\beta - K(S_i)) \sin \varphi_i \end{cases} \quad (*)$$

Where  $W_{ij}$  is the synaptic weight between cells  $i$  and  $j$ ,  $R(S_j)$  is the spike density of the cell  $j$  with sigmoid format:

$$R(S_j) = \frac{1}{2} \left( \tanh(g(S_j - 0.5)) + 1 \right)$$

$$= \frac{1}{2} \left( \frac{\exp(g(S_j - 0.5)) - \exp(-g(S_j - 0.5))}{\exp(g(S_j - 0.5)) + \exp(-g(S_j - 0.5))} + 1 \right)$$

And  $I_i$  is the driving stimulus, selectively activate cell  $i$ . Meanwhile,  $w$  and  $\beta$  are frequency and stabilization coefficient, respectively. The couplings equations of  $C$  and  $K$  are:

$$\begin{cases} C(\varphi_i) = \sigma(\cos \varphi_i - \cos \varphi_0) \\ K(S_i) = \rho S_i \end{cases}$$

with  $\rho$  and  $\sigma$  modulates the coupling and initialize all cells with silent condition ( $S_i = 0$ ) and equilibrium phase  $\varphi_0 = \arcsin(-w/\beta)$  with parameters:  $w = 1$ ,  $\beta = 1.19$  and  $g = 10$  equals to  $-0.997903$ . Furthermore,  $\cos\varphi_0 = .542066$ , the EEG is at 6Hz theta oscillation computed with step changes from 0.01 to 0.1 in simulation, computational time accordingly changes from  $0.01/6/2\pi \sim 0.000265$  to  $0.002653$

Specifically, in single unit:

$$\begin{cases} \frac{dS}{dt} = -S + \sigma(\cos\varphi - \cos\varphi_0) + I \\ \frac{d\varphi_i}{dt} = -w + (\beta - \rho S)\sin\varphi \end{cases} \quad (**)$$

Note that the fixed point attractors are considered only in this paper (process with bifurcation is not considered) since we only compute the direction from excitatory population to inhibitory population while crossing the task networks without stimulus, i.e. TPN-TNN interactions. And  $\rho$  is fixed at 1 while only  $\sigma$  is tuned from 0 to 1 with k5(6 levels in total) in this paper. In addition to the differential equations related to S and  $\varphi$ , the Weight matrix  $W_{ij}$  abbreviated as W can also be defined accordingly and lead to the specific I for each j in neuron i prominently:

$$W(\theta_i - \theta_j) = J^- + (J^+ - J^-) \exp\left(-\frac{(\theta_i - \theta_j)^2}{2\sigma}\right)$$

Where  $\frac{1}{360} \int_0^{360} W(\theta_i - \theta_j) d\theta_j = 1$ ,  $J^-$ ,  $J^+$  is the synaptic strength experimentally and theoretically respectively, leads to the Iext:  $I^{\text{ext}}(\theta, t) = I_0 + I_{\text{cut}} \left( \frac{1 + \cos(\theta - \theta_0)}{2} \right)^p$  at  $p = 2$ ,  $I_0 = 0$  and further I as:

$$I(\theta, t) = I^{\text{ext}}(\theta, t) + \int_{-\pi}^{\pi} \frac{d\theta'}{2\pi} W(\theta - \theta') r(\theta', t)$$

Where the parameter  $\theta$  as the direction of each neuron i,  $\theta_j = 2\pi/N_i$  is evenly distributed covering  $2\pi$ , describing each node in hopfield network (fully connected). Note that the order is fixed and can be changed iff.  $W_{ij}$  are the same for all neurons and the detailed classical computation with normal differential equations is shown in next section while the prominent quantum computation can be found in chapter 2.3(b) and 3.

## 2.2. Approximation with numerical methods on the convert ratio

### a. Gene diffusion referencing bacteria sensing and MTS on difference mapping

As to study the switching model interpreting the process explicitly, we thus combine the deterministic[22] background of the switching between on and off and give out one stochastic model based on the explicit (ordinary differential equation) ODE of the numbers of mRNA and proteins. Although the final model( referencing the quorum sensing model of bacteria in changing environment[23]) removes the dimers but it is used in the first place while cancelled out the in the quasi steady state according to its far more faster production and degradation rate comparing to transcription and translation.(Simplified mechanism sees Figure 1). Start from the bistability of the metastability[24] of the two state model, with the absorbing boundary conditions,  $\rho_0(x^*, t) = 0$  and the identification of mean transition rate with principal eigen value  $\lambda_0 \epsilon$ , the quasi-stationary approximation of

$$\rho_n(x, t) = C_0 * \exp(-\lambda^e t) \varphi \varepsilon^0(x, n)$$

Furthermore, with the quasi-potential satisfying:

$$\sum_{n \in \{0,1\}} S_n(x) (A_n, m(x) + \varphi'(x) \delta n, m) F_m(x) = 0,$$

$$H = 0.5(g_x^2 p_x^2 + g_y^2 p_y^2) + p_1 \varphi_1 + p_2 \varphi_2$$

where  $P_i$  is the momentum conjugate to the generalized coordinate  $x_i$ , where  $g_i = \sqrt{S_{22}^i + X_i/\tau_i}$  (For more specific study of the  $\varphi_1$  and  $\varphi_2$  as the interacted diffusive speed, most studies applies WKB equations.) Since we focus on the transform between two status of the two populations, mRNA (of HS-1)  $X_n$  and proteins Hax1  $Y_n$  as the system. (with dimer  $Z$  of production rate  $k_{XY}$  and degradation rate  $k_P$ ) and the degradation rate of HS1 and hax1, as  $K_X$  and  $K_Y$ , separately. From the original ODES[25]:

$$\frac{dZ}{dt} = k_{XY} XY - k_z Z$$

$$\frac{dX}{dt} = -k_{XY} XY + k_z Z = k_X X + \frac{V_z * Z}{k_X + Z}$$

$$\frac{dY}{dt} = -k_{XY} XY + k_z Z = k_Y Y + \frac{V_z * Z}{k_Y + Z} + X_0$$

where  $X_0$  and  $Y_0$  are the initial volumes or baseline volumes of these two populations and with instant volume as  $V_X$  and  $V_Y$  and due to the zero value of  $dP/dt$ , the term of  $P$  can be replaced through:

$$P = -\frac{K_{XY}}{K_P} * XY$$

$$\frac{dX}{dt} = -\frac{K_X X}{1} + \frac{V_X}{1 + K_X K_P / K_{XY}} + X_0$$

$$\frac{dY}{dt} = -\frac{K_Y Y}{1} + \frac{V_Y}{1 + K_Y K_P / K_{XY}} + Y_0$$

Considering the transform of  $X$  (Upstream only), in the first step as degradation as the first term of right of the upper formula, the degradation part of  $X$  with  $k_X X$  which can be interpreted as the Poisson process and rewrite into  $-\mu_1/\exp(P_X)$ , and in the second term, the coefficient of degradation part of  $X$ ,  $C_1$  is denoted as  $V_X * K_X/\mu_1$ . Mean while with the assumption of continuous Markov chain, where the convert ratio of  $Y$  is  $n$ , the  $k_{XY} * X * Y$  is equivalent to  $(Y/(X+Y))^n$  so that the whole degradation part becomes  $C_1 \mu_1 / (1+(y/(x+y))^n) \exp(P_X)$ ,  $C_2 \mu_2 / (1+(x/(x+y))^n) \exp(P_Y)$ , and the final transform rate of mRNA number  $X$  and proteins  $Y$  are:  $C_1 / (1+(y/(x+y))^n) (\exp(P_X) - 1) - \mu_1 X (\exp(-P_X) - 1)$  and  $C_2 / (1+(x/(x+y))^n) (\exp(P_Y) - 1) - \mu_2 Y (\exp(-P_Y) - 1)$ , where the coefficient of degradation part of  $Y$   $C_2$  denoted as  $V_Y * K_Y/\mu_2$  as the reciprocal of the other population ratio. And as  $Y$  stands for the number of the proteins,  $X$  for the number of the mRNA separately with  $m$  and  $n$  as their translation and transcription rate. With the total sum of the system molecule numbers assumed as  $X+Y$ , we have the Hamiltonian:  $C_1 / (1+(y/(x+y))^n) (\exp(P_X) - 1) - \mu_1 X (\exp(-P_X) - 1) + C_2 / (1+(x/(x+y))^n) (\exp(P_Y) - 1) - \mu_2 Y (\exp(-P_Y) - 1)$ , where  $P_X, P_Y$  are calculated setting  $H = 0$  and  $H_0 = 0$ , and conversion rate which can be calculated as  $dy/dx$ , specifically here, letting the first term equals the second and third equals the fourth term. (Complete see Appendix B) Note that: each single DNA population (hax1 and HS 1) has its own degradation rate when considering about its mRNA computation and the other population's protein is taken as the intake, promoting its population when as normals binding onto the according site of persists, activating it. Vice versa, thus, the two populations have similar structured formula describing each degradation and population under the dual interacted population. The mean switching time is calculated based on the solution of the SDE:  $z' = z + \sqrt{(N_c/N)} \sqrt{1+2*\varepsilon-z} * \eta$ , where  $N_c = 1/\tau$  and  $\eta N(0, \delta)$  is the white noise with correlator  $\langle \eta(\tau) \eta(\tau_0) \rangle = \delta(\tau - \tau_0)$ . Note that it is the span of the master equation in powers of

the inverse population size  $N^{-1}$  re-scaling with  $\tau = 2^{(t/N)}$ , and  $z = x_1 - x_2$  ranges over the interval  $[-1, 1]$  [20], leading to the solution  $\tau_0^* = 2\lambda / (1 - 2\lambda) \cot(\pi)$ . Thus, we have the algorithm:

\*\*\*\*\*

Input: maximum time scale size  $G$ , mRNA numbers  $y$ , proteins  $x$ , maximum steps  $Steps$ , tolerance  $Tol$ , parameters of the sensing model (coefficient of conversion  $c_1, c_2$ , transcription and translation rate  $m, n$ , degradation rate  $k_1, k_2$ , formation coefficients  $\mu_1, \mu_2$ , diffusion rate  $b_1, b_2$ ),  $dt$  as time increment  
 Initialize: maximum time scale,  $T$ , maximum step number  $steps$ , tolerance  $Tol$ , numbers of mRNA after the first diffusion process that if necessary, initialized as one random the number, in the first status we start with the largest interval to cover higher possibilities, i.e.  $[x(0), x(0)+1, \dots, x[1]-1]$ ,

**for do**

**xhat (length(xhat)) < x(i + 1): repeat**

record the size  $T$ , time  $t$ , steps,  $Steps - steps + 1$

set the sequence according to size  $T$  (the interval for mRNA numbers)  $x(1), x(2), \dots, x(T)$  and generate the population number of proteins according data distribution,  $y(1), y(2) \dots y(T)$ .  $T$  initialized as the  $X(i+1) - X(i)$ , consider Hamiltonian Markov (Hierarchical) [26]:

**if** xhat exist (iterated from previous status) **then:**

segment the interval into several sub-sequences ( $X_0$  as the new current status,  $X_1$  as the previous status)

**end if**

**Note that:** As we only consider up streaming, down regulation into those before the previous status is not included.

**Function dynamics inputs:**  $x$  and fixed  $y$  (or  $x_0, y_0$ , or  $x_1, y_1$ )

Calculate degradation term  $w_1$  and  $w_2$  according to the (\*1)

Calculate  $p_x, p_y, dx, dy$ , conversion rate,  $H_e$  and  $H_x, s$  according to Appendix 2 predict multiplied mRNA and protein numbers  $xhat, yhat$ , and other Hamiltonians

Calculate update  $\gamma, \delta$

Calculate tolerance for further stopping criteria as the residue of  $\gamma$  and cell number with:

$tol = \text{abs}(\gamma - \text{gamma}) / \text{gamma};$

$toll = \text{mean}(\text{abs}(xhat - x_1) / x_1 + \text{abs}(yhat - y_1) / y_1)$

**Output:**  $H, Xhat, HthetaX, HthetaY, HxX, HxY, HamilX, HamilY, HamulXhat, HamilYhat, xhat, sX, sY, p_x, p_y, pxhat, pyhat, actionratio, \delta, \gamma, \Delta, \Gamma, cr_1, c_1, c_2, crhat, c_1hat, c_2hat, tol, toll, Txc, Tyc, Txchat, Tychat$

**Concatenate results:**

**If**  $X_0, X_1$  exist then:

$Xhat = [X_0hat, X_1hat];$

**End if**

**If** only  $x_0$  exist then

$Xhat = X_0hat;$

**End if**

Do similar prediction regenerate the mRNA numbers  $X$  according to  $Y$  with

**Function dynamics** again for comparison. Results are with postfix 'L'

Store the quantities of 'successful' moves with smaller tolerance and action for either from mRNA or protein numbers.

**If** satisfies the configuration condition **then**

$Tol = \text{min}(tol + toll, toll + toll);$

**Else**

Fail++

**End if**

.....

## b. Neuron switching in single unit based on normal differential equation

Derived from the equation (\*\*) of single unit fixed point attractors, the normal form around bifurcation point can be computed with:

$$\begin{cases} \frac{dS}{dt} = aS^2 + \lambda_1 S \\ \frac{d\varphi}{dt} = \lambda_2 \varphi \end{cases}$$

In addition to the computation of  $\lambda$  demonstrated in chapter 3 and the regression of the parameters  $q$ , based on experiment data mentioned in 2.1, the global feedback inhibition from the excitatory neurons  $j$  to the single unit  $i$  is depicted as the time series with regards to frequency domain as well through firing rate model and leaky-integrating differential equation:

$$I_i = \tau_i \frac{dI_i}{dt} + \sum_{j=1}^{NI} w_{ij} R(I_j) - G \left[ \sum_{j=1}^{NI} R(I_j) \right] + I_{ext}$$

Where  $R(I_j) = \begin{cases} \ln\left(\frac{I_j}{I_{thre}}\right), & \text{if } I_j > I_{thre} \\ 0, & \text{otherwise} \end{cases}$  (a)

$$G[R(I_j)] = \begin{cases} \sum_{j=1}^{NI} \ln\left(\frac{I_j}{I_{thre}}\right) / NI, & \text{if } I_j > I_{thre} \\ 0, & \text{otherwise} \end{cases}$$
 (b)

Note that, to simplify the computation, among the parameters conductance, eigenvalue of the Jacobian of fixed points and synaptic strength, only the conductance is changed. And the algorithm shows the TNN single unit only here:

\*\*\*\*\*

Input: k5 and prominent conductance for excitatory NMDA gNMDAE, conductance for inhibitory NMDA gNMDAI, conductance for excitatory AMPA gAMPAE, conductance for inhibitory AMPA g AMPAI, conductance for excitatory GABA gGABAE, conductance for inhibitory GABA gGABAI, NI, Iext, time step dt = tao/1000, rest membrane potential Vm, capacitance Cm, leak conductance gL, leak voltage VL, resistance sigma, experimental synaptic strength J-, weight matrix W, neuron direction theta

Initial: t=0, dV\_dt = 0 and I1 = Ithre, in the first status we start from excitatory NMDA(nonselective) to inhibitory GABA populations considering Iext from the excitatory AMPA(selective) and thus we have the  $I_{NMDA}$  controlled by Mg2+ and  $V_E = 0$ :  $I_{NMDA} = \text{sum}(Vm/NI/\text{sum}(1+c\_MG*np.\exp(-0.062*Vm/NI/3.57)))$ ,  $I_{ext} = \text{sum}(\exp(I0)/\text{sqrt}(2pi*sigma)*\exp(-(\text{theta}-\text{theta0})^2/sigma))$ , where theta0 = 0 and theta = [0,2pi/Ni, ...,2pi]

**I.achieve V(t)**

**for do t = 0,dt,...,tao**

1. compute the increase of V each time step:  $dV\_dt = (-gL*(Vm-VL) - I0)/Cm$
2. update  $V(t+dt) = V(t) + dV\_dt = V(t) + (-gL*(Vm-VL) - I0)/Cm$

**end**

**II.achieve Excitatory term Ex and Inhibitory term In and compute simulated I**

**for do t = 0,dt,...,tao**

1. compute increase of I across all cell j to unit i at each time step:  $dIi\_dt = I_{NMDA}$
- for do j = 1,2,...4096**

1. Compute from excitatory status:

$$I_{AMPA\_E,j} = (V(t) - V_E) * g_{AMPAE} * \frac{(1 + \cos(\text{theta}_j - \text{theta}_0))^2}{4}$$

2. Compute from inhibitory status:

$$I_{\text{AMPA}_i} = (V(t) - V_E) * g_{\text{AMPA}_i} * \frac{(1 + \cos(\theta_{i_j} - \theta_{i_0}))^2}{4}$$

$$I_{\text{GABA}_i} = (V(t) - V_E) * g_{\text{GABA}_i} * \frac{(1 + \cos(\theta_{i_j} - \theta_{i_0}))^2}{4}$$

3. Transfer I to firing rate R (according to equation a):

$$R_{\text{AMPA}_E, j}(I_{\text{AMPA}_E, j}), R_{\text{AMPA}_I, j}(I_{\text{AMPA}_I, j}), R_{\text{GABA}_I, j}(I_{\text{GABA}_I, j})$$

4. With weight matrix:  $w_{ij} = \frac{J + (J^+ - J^-) \exp(-\frac{(\theta_i - \theta_j)^2}{2\sigma^2})}{2}$ , compute excitatory term

$$E_X = \sum_{j=1}^{N_I} w_{ij} R(I_j)$$

$$E_X = E_X + w_{ij} * R_{\text{AMPA}_E, j}(I_{\text{AMPA}_E, j})$$

5. Do for inhibitory I: Transfer R to gain G (according to equation b):

$$G[R_{\text{AMPA}_I, j}(I_{\text{AMPA}_I, j})], G[R_{\text{GABA}_I, j}(I_{\text{GABA}_I, j})]$$

6. Compute inhibitory term  $I_n = G \left[ \sum_{j=1}^{N_I} R(I_j) \right]$ :

$$I_n = I_n + G[R_{\text{AMPA}_I, j}(I_{\text{AMPA}_I, j})] + G[R_{\text{GABA}_I, j}(I_{\text{GABA}_I, j})]$$

7. Compute  $dI_i/dt = dI_i/dt + I_{\text{AMPA}_E, j}$

end

2. Compute the total I at time t:  $I_i(t) = \tau_i * dI_i/dt + E_X - I_n + I_{\text{ext}}$

end

Output:  $I_i(t)$ ,  $dI_i/dt$ ,  $E_X$ ,  $I_n$

\*\*\*\*\*

## 2.3. Stochastic Model for (a) gene switches

### 2.3.1. Probabilistic Uncertainty Conditional

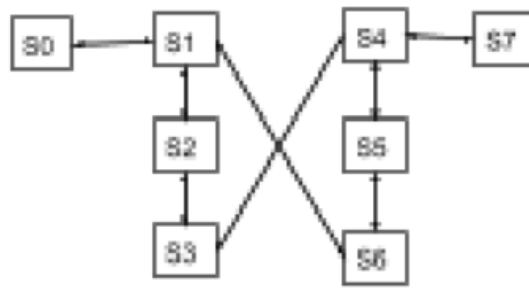


Figure1: Belief Graph

Where  $S_0 = \text{hax1\_DNA}^{\text{inactive}} \wedge \text{hax1\_DNA}^{\text{low\_concentration}}$

$S_1 = \text{hax1\_DNA}^{\text{active}} \wedge \text{hax1\_DNA}^{\text{high\_concentration}}$

$S_2 = \text{hax1\_mRNA}^{\neg\text{degrade}}$

$S_3 = \text{hax1\_protein}^{\neg\text{degrade}}$

$S_4 = \text{HS1\_DNA}^{\text{inactive}} \wedge \text{HS1\_DNA}^{\text{low\_concentration}}$

$S_5 = \text{HS1\_mRNA}^{\text{active}} \wedge \text{HS1\_DNA}^{\text{high\_concentration}}$

$S_6 = \text{HS1\_mRNA}^{\neg\text{degrade}}$

$S_7 = \text{HS1\_protein}^{\neg\text{degrade}}$

Transition rate[27]: R/P (R for CTMC, P for DTMC)

### 2.3.2. Model Check for Stochastic Models Combining Continuous Time Markov Chain with Embedding in Reward Computation

The logic applied on a probabilistic notion regards to the belief graph is based on the trust which is reflected by the reliability and predictability. Specifically, the language of the stochastic models used for computing CTMC [28] is the Continuous Stochastic Logic (CSL) developed and extended by some research

A CTMC is a tuple  $C = (S, s, R, L)$  where  $S$  is the finite set of states,  $s$  is the initial state;  $R$  is  $S \times S \rightarrow R \geq 0$  is the transition rate matrix;  $L: S \rightarrow 2AP$  is a labelling function which assigns to each state  $s \in S$  is the set  $L(s)$  of atomic propositions valid in the state. Instead of the case of DTMCs, a fixed set of atomic propositions  $AP$  is applied, the transition rate matrix  $R$  assigns rates to each pair of states in the CTMC, used as parameters of the exponential distribution. A transition can only occur between states  $s$  and  $s'$  if  $R(s, s') > 0$ , representing the probability of this transition being triggered within  $t$  time-units equals  $1 - e^{-R(s, s')t}$ . Time spent in state  $s$ , before such transition occurs, is exponentially distributed with rate  $E(s)$ , where:  $E(s) = \sum(R(s, s'))$ , where  $E(s)$  is known as the exit rate of state  $s$ .

The embedded DTMC of a CTMC, is the probability of each state  $s'$  transitioned from the previous  $s$ , independent of the time, defined as:

$\text{Emb}(C) = (S, s, P_{\text{emb}}(C), L)$  where for  $s, s' \in S$ :

$$P_{\text{emb}}(C)(s, s') = \begin{cases} R(s, s') / E(s), & \text{if } E(s) \neq 0 \\ 1, & \text{if } E(s) = 0 \text{ and } s = s' \\ 1, & \text{otherwise} \end{cases}$$

where the behavior of the CTMC in the alternative way remains in a state  $s$  delayed and exponentially distributed with rate  $E(s)$  and transit with  $P_{\text{emb}}(C)(s, s')$ .

The infinitesimal generator matrix for the CTMC  $C=(S, s, R, L)$  is the matrix  $Q: S \times S \rightarrow R$  defined as:

$$Q(s, s') = R(s, s'), \text{ if } s \text{ is not } s' - \sum_{s'' \neq s} R(s, s'') \text{ otherwise}$$

The CTMC stores the transition from  $s$  to  $s'$  in ratio format instead of the possibility in DTMC.

However, the probability measures  $\text{Pr}_s$  on  $\sum \text{Path}_C(s)$  as the unique measure such that  $\text{Pr}_s(C(s)) = 1$  and for any cylinder  $C(s, I, \dots, I_{n-1}, s_n, I', s')$ ,  $\text{Pr}_s(C(s, I, \dots, I_{n-1}, s_n, I', s'))$  equals:

$$\text{Pr}_s(C(s, I, \dots, I_{n-1}, s_n)) = \text{Pr}_s(C(s, I, \dots, I_{n-1}, s_n)) * P_{\text{emb}}(C)(s_n, s') (e^{-E(s_n) * \text{infl}' - e^{-E(s_n) * \text{supl}'})}$$

In our case, such model check as with PCTL, we can easily derive the path formulae for the states between  $S_0$  and  $S_7$  separately with 6 time intervals  $I = [t_0, t_i]$ :

$$P \sim p[\diamond I \varphi] = P \sim p[\text{true} U I \varphi],$$

$P \sim p[\diamond I \varphi] = P \sim p[\text{exist } U I \varphi]$ ,  $\varphi =$  'transit, Stands for the probability that a transition occurs in time interval  $I = [t_0, t_i]$ , And thus, For determining the least solution,

$$\text{Prob}_C(s, \varphi, U[0, t], \psi) = \int \sum P_{\text{emb}}(C)(s, s') * E(s) * e^{-E(s) * x} * \text{Prob}_C(s', \varphi, U[0, t], \psi)$$

$$= \text{ProbC}(\varphi, U[t, \infty]) = \text{Prob}\{\text{ProbC}(s, \varphi, U[0, t' - t], \psi), \text{if } s| = \varphi \text{ otherwise}\}$$

And define the rewards function a CTMC  $D=(S,s,R,L)$ , the semantics is defined as:  $S \models R \sim r[I=t], \text{ExpC}(s, XI=t) \sim r$

### 2.3.3. Model Check for Stochastic Models reachability/safety computing based on Discrete Time Markov Chain(DTMC) approximating the Discrete Time Markov Process(DTMP)

In the second application of model check, the continuous dynamics described by switching diffusions is studied with reachability and dually safety properties on DTMC. Compared with the MC on continuous time domain, DTMC is defined with a fixed, finite set of atomic propositions used to label states. The DTMC  $D$  is a tuple similar as CTMC  $(S,s,P,L)$ , where  $S$  is a finite set of states;  $s$  is the initial states;

$S^*S \rightarrow [0,1]$  is the transition probability matrix where  $\sum_s P(s,s') = 1$  for all  $s \in S$  where  $L(s)$  of atomic propositions are valid.

$$(\max\{dq(t1, t2)\} \leq Kd * |t2 - t1|.)$$

and  $K \geq 12$  is the Dudley metric universal constant. Let  $h$  defined larger than 0 be a sampling time and the mean  $E$  and the covariance  $C$  to simulate a normal distribution  $N(x|E,C)$ . Then, the discrete kernel is

$$\begin{aligned} T((A, qj), (x, qi)) &= \int AN(x|eF(qi) * hx, \text{gamma}(I, h)) dx * e^{-\bar{A}h} \quad \text{if } qi = qj \\ A(\int N(x|Eqi, x(s), C qi, x(s)) dx * \text{lambda} * \bar{A}ij / \bar{A}i * \bar{A}i * h * e^{-\bar{A}h}) &\text{ if } qi = qj, \\ ((A, qj), (x, qi)) &= \int AN(x|eF(qi) * hx, \text{gamma}(I, h)) dx * e^{-\bar{A}h} \quad \text{if } qi = qj \\ \text{Where } \text{gamma}(i, t) &= \int A(eF(qi) * (t - m)) * G(qi) * G(qi)T(eF(qi) * (t - m))T dm \\ \bar{A}i, \bar{A}i, t(s) &= (\bar{A}i - \bar{A}i) * e^{(\bar{A}j * s - \bar{A}i * t - Ai * s)} / (e^{\bar{A}j * s} - e^{\bar{A}j * s}), \\ Eqi, x(s) &= eF(qi) * s * eF(q) * (h - s) * x, Cqi, x(s) \\ &= eF(qi) * s * \text{gamma}(i, t) * eF(q) * (h - s) * x + \text{gamma}(j, h - t), \\ 0 \leq \text{eps} \leq 1 - e^{-\bar{A}i * h} - \bar{A}i * h * e^{-\bar{A}i * h}, \end{aligned}$$

With the events on  $t$  belongs to  $I$ ,  $A_n = \{X(t) \in S | P \sim p[1, ] = P \sim p[\text{true UI } \varphi]\}$ ,  $B_n = \{X(t) \in S | P \sim p[\neg I \varphi] = P \sim p[\text{exist UI } \varphi]\}$ ,  $P_{\text{safe}}(X, S, I) = \lim P(A_n \wedge B_c)$ ,  $P_{\text{reach}}(X, S, I) = 1 - \lim P(A_n \wedge B_c)$

$$\begin{aligned} \int \sum T dx(z1, z2) &= T(z1, z2), \text{ if } z1, z2 \in S \text{ dx} = 1 - \sum_{zj \in S} dx zT(z), \quad \text{if } z1 \in S \text{ dx}, z2, z2 \in S \\ &= -1, \quad \text{if } z1, z2 \in \varphi, \\ &= 0, \quad \text{if } z1 \in \varphi, z2 \in S \text{ dx} \end{aligned}$$

Continuous kernel proof see Appendix B.

To compute the reachability/safety properties, we introduce the scheme based on Discrete Time Markov Chain(DTMC) which discretize the state space to approximate the Discrete Time Markov Process(DTMP) results from the original switching diffusion process  $H$ , a tuple  $H=(Q, K, F, G, W, \wedge)$ , where  $Q = \{q1, \dots, q|Q|\}$  is the set of discrete modes instead of the matrix in CTMC and  $Y=(X, \alpha)$  its solution. For any  $q \in Q$ , call  $X_q$  the solution of the SDE :  $X_q(t) = F(q) * X_q(t) dt + G(q) * dW(t)$  (\*) In this section we assure that  $X_q$  is a  $u_i$ -dimensional, zero mean Gaussig, an process (GP).  $X_q$  is almost surely bounded within the interval  $I$  by Assumption. Set  $h = \min\{2(-n)/(2 * \sqrt{(2) * K2 * Kd}), 2^{-n}\}$  and  $\epsilon_n = 2(-n/2)$ , where  $n \in \mathbb{N}$ , and  $Kd$  is a constant such that for any  $t1, t2 \in I$

### 2.3. Quantum Computation Model for (b)neuron spikes

In accordance with classical computation, we use the entanglement of two neutral atoms  $x_1, x_2$  (fast two-qubit gates) to compute the transmission between two eigenstates here denoted as  $|g\rangle$  and  $|e\rangle$ , alternatively  $|0\rangle$  and  $|1\rangle$ . Hamiltonian holding time and position information is utilized to express the interactions similarly separated into internal and external parts:

$$H(t, x_1, x_2) = H_{\text{ext}}(t, x_1, x_2) + H_{\text{int}}(t, x_1, x_2)$$

Briefly,  $H_{\text{ext}}$  can be spanned from dipole-dipole interaction around distance  $r = |x_1 - x_2|$  and the photon kick[22] happened during absorption from  $|g\rangle$  to Stark eigenstate  $|r\rangle$ [21]. We focus on the internal interactions mainly with phase gates with internal dynamics induced by the standard Hamiltonian:

$$H^i(t, x_1, x_2) = u|r\rangle_1\langle r| \otimes |r\rangle_2\langle r| + \sum_{j=1,2} [(d_j(t) - i\gamma)|r\rangle_j\langle r| - \frac{\Omega_j(t, x_j)}{2} (|g\rangle_j\langle r|)]$$

Where  $d(t)$  detunings and  $\Omega_j(t, x_j)$  Rabi frequencies describes the exciting lasers while  $\gamma$  accounts for decay from the excited states  $|r\rangle$ .

Next, we focus on the transfer of the system with the Hamiltonian:

$$H = \sum_{a,b} H^{a,b} \otimes |a\rangle_1\langle a| \otimes |b\rangle_2\langle b|$$

Where  $H^{a,b} = \sum_{i=\{a,b\}} \left[ \frac{p_i^2}{2m} + V^i(x_i, t) \right] + u^{a,b}(x_1 - x_2)$  with  $p_i$  being the momentum operator.

Each single unit of neuron model can be seen as one single state either being excitatory or inhibitory analogue to the logical states  $|1\rangle$  or  $|0\rangle$  and the direct switching equals to the entanglement with energy shift while:

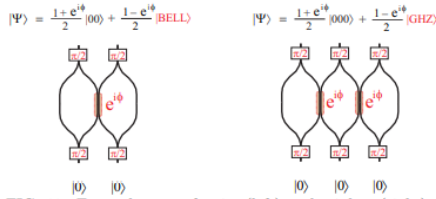


FIG. 10. Entanglement of pairs (left) and triplets (right) of neighboring atoms by a single lattice shift.

Specifically, one obtains the following transformations. For isolated atoms:

$$|0\rangle \rightarrow |0\rangle;$$

for pairs of neighboring atoms:

$$|00\rangle \rightarrow \frac{1+e^{i\phi}}{2}|00\rangle + \frac{1-e^{i\phi}}{2}|BELL\rangle;$$

and for triplets of neighboring atoms:

$$|000\rangle \rightarrow \frac{1+e^{i\phi}}{2}|000\rangle + \frac{1-e^{i\phi}}{2}|GHZ\rangle;$$

where we have used the notation

$$|BELL\rangle = \frac{1}{\sqrt{2}}\{|0\rangle|+\rangle - |1\rangle|-\rangle\},$$

$$|GHZ\rangle = \frac{1}{\sqrt{2}}\{|0\rangle|+\rangle|1\rangle - |1\rangle|-\rangle|0\rangle\},$$

Basically, the truth table can be achieved through the fundamental phase gate:

$$|0\rangle|0\rangle \rightarrow |0\rangle|0\rangle$$

$$|0\rangle|1\rangle \rightarrow |0\rangle|1\rangle$$

$$|1\rangle|0\rangle \rightarrow |1\rangle|0\rangle$$

$$|1\rangle|1\rangle \rightarrow e^{-in(-2\varphi_r^{ab} + \varphi_r^{bb})}|b\rangle_1|b\rangle_2$$

applying a single-bit rotation:

$$|0\rangle \rightarrow |0\rangle e^{-i\varphi_r^a} + |1\rangle e^{-i(\varphi_r^a + \varphi_r^{ab})}$$

Further more, in such a scheme, a NI-bit code where the codewords:

$$|0s\rangle = (|000\rangle + |111\rangle)/\sqrt{2}^3$$

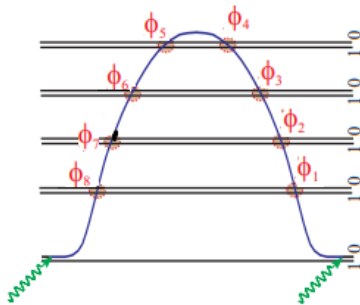
$$|1s\rangle = (|000\rangle - |111\rangle)/\sqrt{2}^3$$

Composed by GHZ states[23], embed the 2D qubit's Hilber space into  $2^{NI}$

D qubit's Hilber space:

$$\mathcal{H} \ni \alpha|0\rangle + \beta|1\rangle \mapsto \alpha|0s\rangle + \beta|1s\rangle \in \mathcal{H}_E \subset \mathcal{H}^{\otimes 9}.$$

Another entanglement is to transport the state  $|r\rangle$  excited from either  $|0\rangle$  or  $|1\rangle$  and then move the lattice:



With a selected atom in the state  $(|0\rangle + |r\rangle)$  onto a string of NI atoms in  $(|0\rangle + |1\rangle)^{\otimes NI}$ , we can see the sweep entanglement as moving the transport lattice to sweep the selected atom across the N lattice and transform the state of atoms onto  $e^{i\varphi^0}|0\rangle + e^{i\varphi^1}|1\rangle$

with  $\varphi = \varphi^1 - \varphi^0$  a differential phase and result to the resulting state:

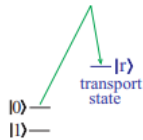
$$|0\rangle (|0\rangle + |1\rangle) \dots (|0\rangle + |1\rangle) +$$

$$|r\rangle e^{iN\varphi^0} (|0\rangle + e^{i\varphi}|1\rangle) \dots (|0\rangle + e^{i\varphi}|1\rangle)$$

For  $\varphi = \pi$ , the GHZ on N+1 dimension can be swept to the standard form:

$$|\psi\rangle = \frac{1}{\sqrt{2}} (|0\rangle|0\rangle|0\rangle \dots |0\rangle + |1\rangle|1\rangle|1\rangle \dots |1\rangle)$$

with one operation.



### 3. APPLICATION AND RESULTS

To have a clearer understanding of the switching process combining the binding with increasing and decreasing speed both of  $hax1$  and  $HS1$ , the two population are regarded as promoters and resistors both when activating and deactivating each other's production. (The coarse process can be briefly described as in figure 2, and it is briefly introduced in the previous chapter.)

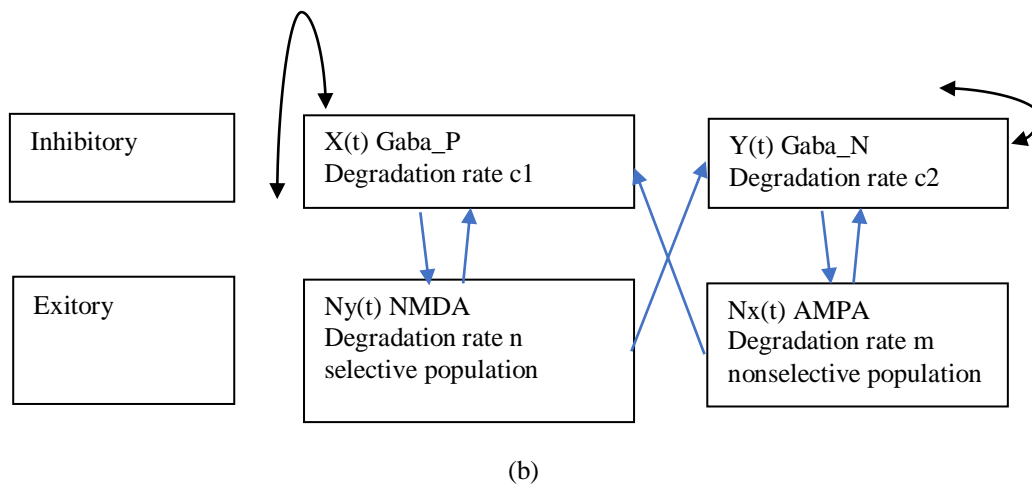
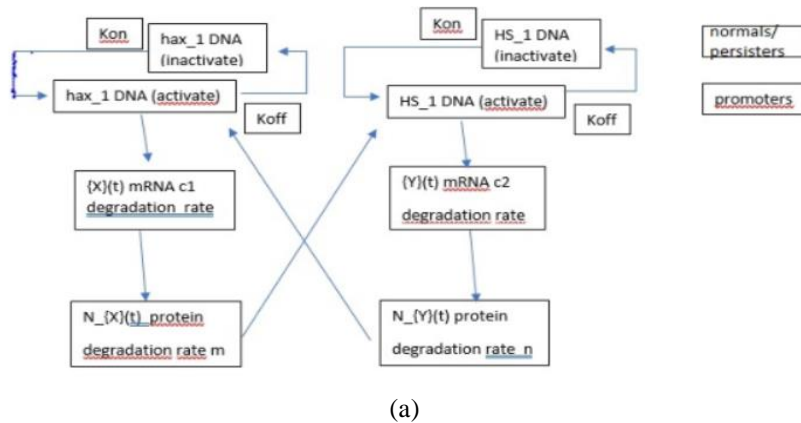


Figure 2: Pipeline for (a) top: gene model; (b) bottom: neuron model

### 3.1. Stability Analysis

#### a. Three critical points for the gene model

As we have data (see Appendix C) of 15 status in all both for hax1 and HS 1 with their different cell numbers taken as X and Y in our model. For reward computation for their Markov chain, we pre-compute the their Hamiltonians, Action Potentials, mean switching time and related dynamics in the form (see availability), and the 6upstreaming status, which is the focus of the experiment application of our model. Using the pre-computation results, we are able to discuss about some practical problems about the current model. There are three groups of quantities studied combining the action potential as well as Hamiltonian inspired by bacterial quorum sensing, 'momentum and cell numbers', 'MTS with the SDE', and 'corresponding Hamiltonians', of each transform status in Appendix A.

First, we use the Taylor expansion to simplify the four ODE achieved in Appendix B: to

$$\begin{aligned}
 dx &= C1 / (1 + (y/(x+y)) mPx - \mu 1 * x * PX) \\
 dy &= C2 / (1 + (x/(x+y)) nPY - \mu 2 * y * PY) \\
 dPx &= C2m(x/(x+y)m - 1 / (1 + (x/(x+y)m)^2 (PY - 1) - \mu 1 * Px - \mu 1 \\
 dPY &= C1n(y/(x+y)n - 1 / (1 + (y/(x+y)n)^2 (PX - 1) - \mu 2 * PY - \mu 2
 \end{aligned}$$

Note that our model here simplify the origin model where  $C_i = a_i/b_i$ , with  $b_i = 1$  as the burst size of protein  $i$ ,  $x/(x+y) = x/(K_2*(x+y))$  as  $k_2 = 1$  is the dissociation constants standing for gene  $x$  binding on  $y$ 's protein binding site. Regarding  $x$  and  $y$  as leading order variable, we apply phase analysis to consider the solution's stability around the three zero-energy points, which achieved through setting  $dx$ ,  $dy$ ,  $dP_X$  and  $dP_Y$  all to zero and combine the Hamiltonian's special case when  $H = 0$  (and  $H_P = 0$ ):  $P_1(x, y, \mu_2*X/C_1, \mu_1*Y/C_2)$ , where  $x$  and  $y$  are the solution of  $x = C_1\mu_1*(1+(y/(x+y))^n)$  and  $y = C_2\mu_2*(1+(x/(x+y))^m)$ ,  $P_2(x, y, 0, 0)$ , where  $x$  and  $y$  are the solution of  $x = C_1\mu_1(1+(y/(x+y))^n) = -y = -C_2\mu_1(1+(x/(x+y))^m)$ , and  $P_3(0,0,0,0)$ . As  $P_X$  and  $P_Y$  are either zero or formula can be replaced by  $x$  and  $y$  around those three convergence points. We here, consider the analysis on  $x$  and  $y$  as following: denote  $dx = f(x,y)$  and  $dy = g(x,y)$ , and the we try to find  $x^*$  and  $y^*$  satisfy the  $f(x,y) = 0$  and  $g(x,y) = 0$  as well as holding the zero-energy points for their momentum. Thus with approximation:  $dx = f_X(x^*,y^*)(x-x^*) + f_Y(x^*,y^*)(y-y^*)$ , and  $dy = g_X(x^*,y^*)(x-x^*) + g_Y(x^*,y^*)(y-y^*)$ . We have

$$A = \begin{pmatrix} f_x & f_y \\ g_x & g_y \end{pmatrix} \\ = \begin{pmatrix} -u_1 P_x & \frac{C_2 n \left[ \frac{y}{x+y} \right]^{n-1}}{\left( 1 + \left[ \frac{y}{x+y} \right]^n \right)^2} P_x \\ -u_2 P_y & \frac{C_1 m \left[ \frac{y}{x+y} \right]^{m-1}}{\left( 1 + \left[ \frac{y}{x+y} \right]^m \right)^2} P_y \end{pmatrix}$$

Where there exists the  $a > 0$ ,  $b > 0$  for the eigenvalue  $\lambda$ :

$$\lambda^2 + a\lambda + b = 0 \quad (1)$$

$$a = -(f_x + g_y) | (x^*, y^*) \quad (2)$$

$$b = |A| \quad (3)$$

so that point  $(x^*, y^*)$  is the convergence points. Thus, we discuss about the stability of the three points as following: we denote  $X = (1 + (x/(x+y))^m)$  and  $Y = (1 + (y/(x+y))^n)$ , compute the  $a$  and  $b$  as:

$$= \mu_1 * P_x + \frac{-(f_x + g_y) | (x^*, y^*)}{\left( \left( 1 + \frac{x}{x+y} \right)^n \right)^2} = |A| | (x^*, y^*) \\ = u_2 * P_x * P_y * C_1 n \left( \frac{\frac{y}{(x+y)^{n-1}}}{\left( 1 + \frac{y}{x+y} \right)^n} \right)^2 \\ - u_1 P_x P_y C_1 m \left( \frac{x/(x+y)}{\left( 1 + x/(x+y) \right)^n} \right)^2$$

[1] for  $P_1 \left( x, y, \mu_1 \frac{2x}{C_1}, \mu_1 * P_x * P_y * \frac{C_2 m \left( \frac{x}{x+y} \right)^{m-1}}{\left( 1 + \frac{x}{x+y} \right)^n} \right)$ , where  $x$  and  $y$  are the solution of  $x = C_1/u_1(1 + (y/(x+y))^n)$  and  $y = C_2/u_2(1 + (x/(x+y))^m)$ .

$$a = \mu_1 * u_2 * \frac{x}{C_1} + \mu_1 * y * \frac{C_2 m \left( \frac{x}{x+y} \right)^{m-1}}{\left( \left( 1 + \frac{x}{x+y} \right)^n \right)^2}$$

$$= \mu_2^2 * B^2 + \mu_1 * C_2 * A * m * (x/(x+y))^{(m-1)}/\mu_2 * A * B,$$

[2] Thus, for  $P_2$ ,  $a = b = 0$ . It's unstable.

[3] for P3 (0, 0, 0, 0), same as P2, a = b = 0 and it's unstable.

**b. Two fixed points for the neuron model**

When there is no stimulus, the neuron fire spontaneously(I=0),  $w < \beta$ , the two fixed points is studied through  $\mu (= \rho\sigma)$  changing with  $\sigma$ :  $M0 = (0, \varphi_0) = (0, \arcsin(-w/\beta)) = (0, -0.997903)$  and  $M1 = (S1, \varphi1) = (1, \pi/2 - \arcsin(-w/(\beta - \rho S0))) = (1, 2.568699)$ .

Similar to the model a, we denote  $f(S, \varphi) = -S + \sigma(\cos\varphi - \cos\varphi_0) + I$ ,  $g(S, \varphi) = w + (\beta - \rho S)\sin\varphi$  and the stability of M0 is linear thus can be analysed with the Jacobian of the coupled (\*\*\*) at  $\varphi_0$ :

$$A = \begin{pmatrix} f_s & f_\varphi \\ g_s & g_\varphi \end{pmatrix} = \begin{pmatrix} -1 & -\sigma \sin(\varphi_0) \\ -\rho \sin(\varphi_0) & \beta \sin(\varphi_0) \end{pmatrix} = \begin{pmatrix} -1 & \frac{\sigma}{1.19} \\ \frac{1}{1.19} & \frac{1}{1.4161} \end{pmatrix}$$

we try to find  $S^*$  and  $\varphi^*$  satisfy the  $f(S^*, \varphi^*) = 0$  and  $g(S^*, \varphi^*) = 0$  as well as holding the zero-energy points for their momentum. Thus with approximation:  $dS = f_s(S^*, \varphi^*)(S - S^*) + f_\varphi(S^*, \varphi^*)(\varphi - \varphi^*)$ , and  $d\varphi = g_s(S^*, \varphi^*)(S - S^*) + g_\varphi(S^*, \varphi^*)(\varphi - \varphi^*)$ . Where there exists the  $a > 0, b > 0$  for the eigenvalue  $\lambda: \lambda^2 + a\lambda + b = 0$ . Thus,  $a = -(f_s + g_\varphi)|_{(S^*, \varphi^*)} = -1 + \beta \sin(\varphi^*) = -2$ ,  $b = |A| = -(\beta \sin(\varphi^*) + \sigma \sin(\varphi^*) \rho \sin(\varphi^*)) = -(-w + \mu c (w/\beta)^2) = -0.323219$ , leading to  $\lambda = 0.5 * (\eta - 1 \pm \sqrt{(\eta - 1)^2 + 4(\rho\sigma \sin(\varphi_0)^2 + \eta)}) = \{0.817465, -1.361948\}$ ,  $\mu_c = 0.95839$

- [1] M0 is stable fixed-point for  $\mu < \mu_c$ , M1 is unstable with  $\varphi1 > \varphi0$  and  $S1 > S0$
- [2] M0 is attractor for  $\mu = \mu_c$ , another fixed point  $M1 = M0$
- [3] M0 is unstable fixed-point for  $\mu > \mu_c$ , M1 is stable with  $\varphi1 > \varphi0$  and  $S1 < S0$

On quantum field, short introduction about two Rydberg here is covered for comparison.

[1]  $u \ll \Omega_j$  makes it unnecessary to address two atoms separately. Because  $\Omega_1 = \Omega_2 = \Omega$ , we can set  $d1 = d2 = 0$  and realize the gate with a)drive a pi-pulse to two atoms->b)pause for  $dt = \varphi / u$ ->c)drive a pi-pulse again to two atoms. Note that the accumulated phase is sensitive to atomic distance and the decay probability is approximately  $p_l = 2 \varphi \Upsilon / u$

[2] Adiabatical condition for  $u \gg \Omega_j$  still makes it unnecessary to address two atoms separately. As  $\Omega_1 = \Omega_2 = \Omega$ ,  $d1 = d2 = 0$  naturally hold due to the slow on time scale given by the two parameter although larger than trap oscillation frequency. The detuning includes a Stark shift as connected to initial state  $|gg\rangle$  with energy  $e_{gg}(t) = \text{sgn}(d)(|d| - (d^2 + 2\Omega^2)^{1/2})/2$  driven adiabatically, where  $d = d - \Omega^2/(4d + 2u)$  while  $|eg\rangle$  and  $|ge\rangle$  are achieved with  $e_{eg}(t) = \text{sgn}(d)(|d| + (d^2 + \Omega^2)^{1/2})/2$  leading to the entanglement phase to be  $\varphi(t) = \sum_{i=0}^n dt i'(e_{gg}(t_i) - 2e_{eg}(t_i))$ .

[3]  $u \ll \Omega_j$  generally requires the atoms to be set differently at  $\Omega_1, \Omega_2$  differently. But we can still set  $d_j = 0$  with the cost of sign change in the wave function through a)drive a pi-pulse to the first atom->b)a 2pi-pulse to the second c)drive a pi-pulse again to the first atom.

### 3.2. Dynamics Analysis

#### a. HMC dynamics for protein and mRNA

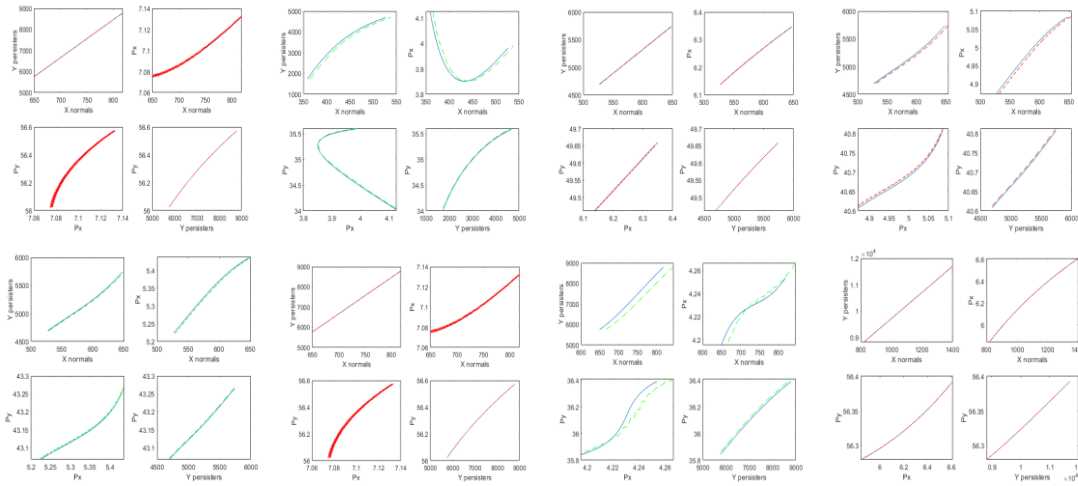


Figure 3(a)-(h) transition between mRNA and protein

In the second part here, with regard to the detailed behavior of mRNA and protein dynamics, we look into their momentum and numbers with 6 status (only the first 2(a)-2(c) and the last 2(d)-2(f) transition examples of the origin 3 groups \* 5 transition statuses figures) in all are studied detailedly while the whole data based on 15 status. As we only investigated the positive direction, the red ones (top left) the application on clinical data while green one (top right) in the larger scaled simulation with more transition status (blue dashed line is the predicted dynamics). Note that the persisters and normals are the roles they take in the whole process (considering from bifurcation to catastrophe and extinction) where here they can be all considered as promoters as their numbers both grows in this process until the last status as their interaction in constant environment is of our main interest as we mentioned before. Generally, with small change studied in one status, the trend is more significant than the larger scale transition. For instance, the green simulation are always more sensitive to the momentum change and shows them more significantly on the cell trajectory comparing to the red clinical transition (we manually break one clinical status into sub-status in simulations.)

Specifically, in the 1- > 2 transition, the production of the HS 1 is slightly faster than hax1 with the accelerate from faster to slower as well as the hax1 0 s momentum decreases from fast to slow while HS 0 1 s momentum increases from fast to slow similarly. The larger scaled simulation show the trend similarly but with larger momentum difference and thus gives out the curve trajectory instead of straight line in the top left figure; On contrary, in 2- > 3 transition, both the clinical application and larger simulation give totally the same behavior according to the dynamics, where proteins products faster than mRNA but with similar acceleration. Other transition can be similarly analysis. Note that from the 4- > 5 of the larger scale simulation, there starts to show the switching where the protein changes into persisters with degradation instead of production which can be both detected from cell numbers figure in the top left and momentum figures in the right bottom although the fewer status contained clinical data does not show this behavior yet. In the last transition status, the switching of proteins becoming into persister is detected in both clinical process and simulation, where in the clinical data, the momentum change of roteins and mRNA are both linear process while in simulation, the momentum of the mRNA grows slightly from faster to slower and proteins degradate slightly from faster to slower as well

and in the last short time, proteins go back to normals again which according to the rising number change in the top left and increase in the momentum both relatively to mRNA(left bottom) and absolutely (right bottom.)

In the second series of figures 2(c), 2(f), we compute the mean time to switch approximation with the solution based on mapping to their difference space where we choose the object as 1) single population of mRNA to the end of the transition (top left); 2) single population of proteins to the end of the transition (top right); 3) mRNA population to the end status of protein (left bottom) and 4) proteins population to the end status of mRNA (right bottom.) There gives some different patterns, as in the 1- > 2, both the mRNA and proteins has the mean time to switch increase linearly with their number change while there exists one significantly longer time at 0.4 for the proteins compare to the final status of mRNA and one totally unstable transition recorded; In the 2- > 3, all the MTS increase linearly with the cell number growth; In the 4- > 5, as there exists the decrease of proteins thus there exists one negative MTS stands for the status; And in 5->6, the last status for the proteins again, compared to the final status where the number back to increase, the previous degradation status also leads to the minus MTS but positive to the mRNA as they both grow in the end. In the last part, Further application using the transition matrix of the model, we compute some basic markov chain quantities based on the stochastic process as following with the pre-computation result (in availability):

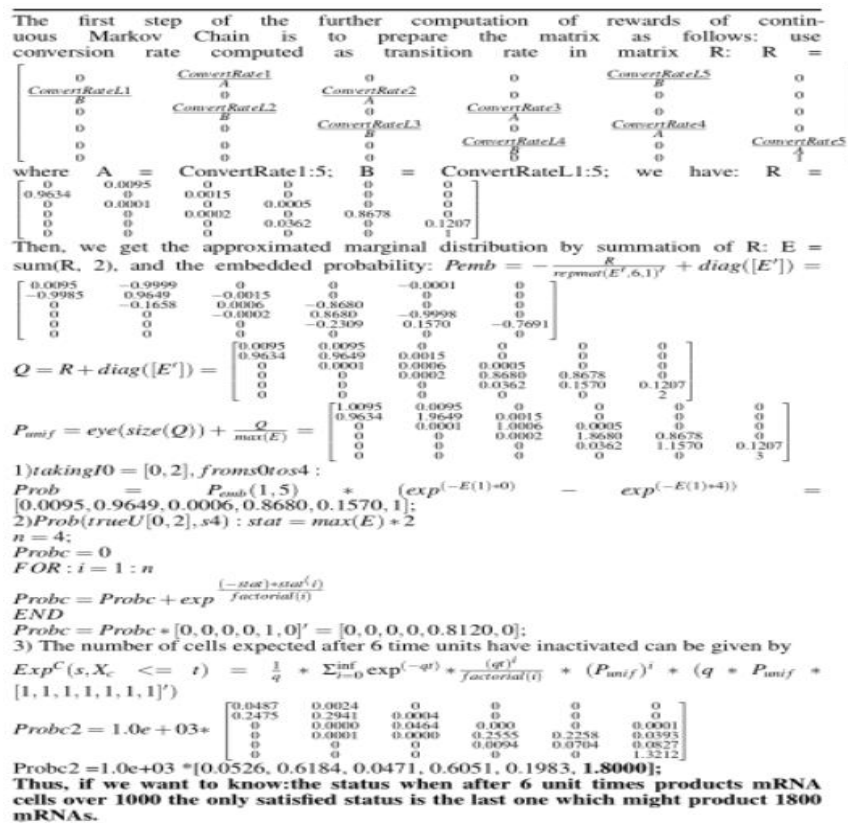


Figure 4 computation of probabilistic safety

In the probabilistic safety computation by finite DTMC abstraction, the computation is based on the differential cognitive (\*) in 2.3.3 with the previous unified matrix of CTMC composed of 6 transition status and 6 time points for each,  $dX = P(:, 2:6) = P(:, 1:5)$ ;

Continue the error bounds for time discretization in 2.3.3, considering mean:  $\mu = \text{mean}(P,1)$ ;  $\sigma^2 = \text{var}(P,1)$ ;  $\sigma = \text{std}(P,1)$ ;  $W \sim N(\mu, \sigma^2) = \text{repmat}(\text{ones}(1,6) ./ \sqrt{2 * \pi * \sigma^2}, 6, 1) * \exp(-\text{repmat}(\mu, 6, 1) .^2 / 2 ./ \text{repmat}(\sigma.^2, 6, 1))$ ; Then the Brownian,  $G = \exp(\mu .* t - \sigma.^2 .* t / 2 + \sigma .* W)$ ; With  $d = \sqrt{(X)^2}$ , As  $dt = 1$  fixed,  $Kd = \max(d) = 1.3433$ ; And with sampling time  $h = \min(2(-6)/\sqrt{2})/Kd, 2(-6)) = 0.28558$

Finally, with  $I = 0:5, Pds = T, z_0 = 1$ , we can achieve:

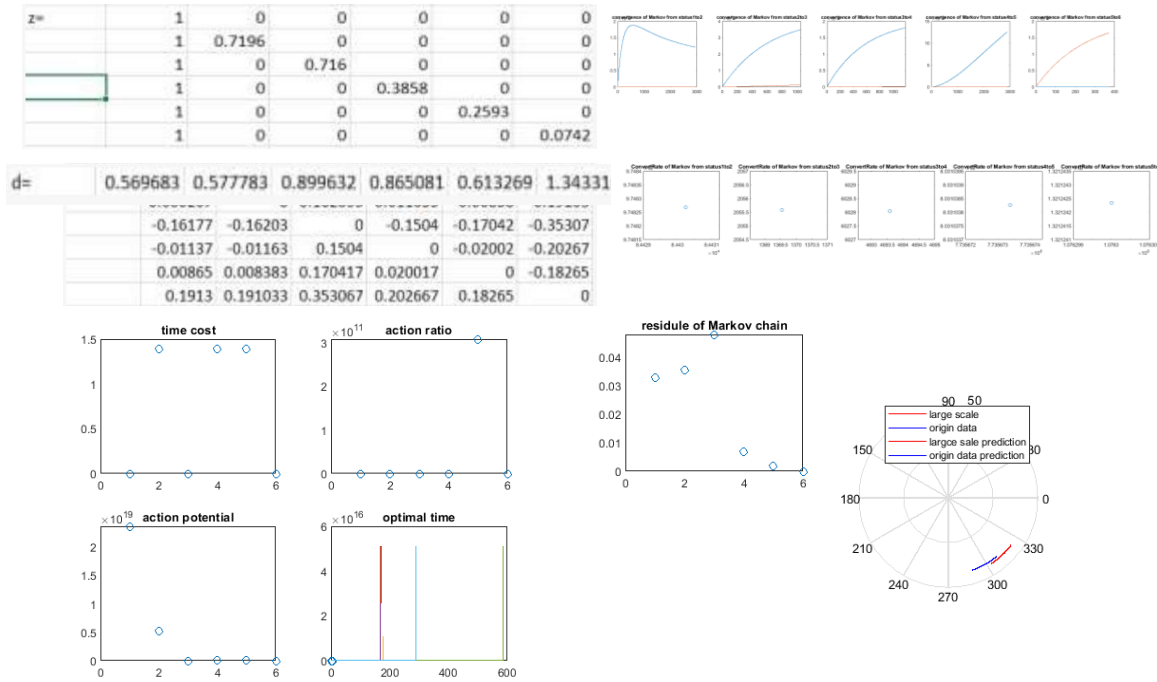


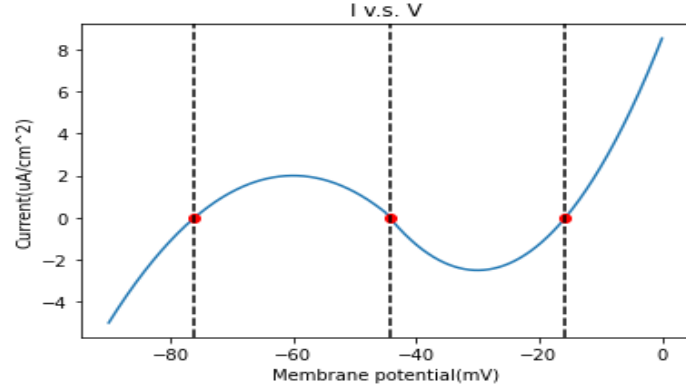
Figure 5. (i) convergence of MC; (j) convert rate from low I to i+1 level (k) total metrics related to time domain; (l) residue of Markov Chain and phase.

### b. Application on neural network oscillation model analogue to computation on quantum computer with all versus-nothing arguments

Specifically, we apply the model on neurons. Considering the energy computation, the flow of ions crosses the membrane, associating the oscillations and construct the up-states and down-states with the interactions in the network. Although coupling of neurons are specific to event/task, to simplify, we adopt the Hopfield network instead (the weight connecting two states is symmetry:  $w_1 = w_2 = w$ ).

Classically, we start with one unit,  $V_i = V, C_{Mg} = 1$ , steady state ( $V_E = 0$ ) I-V curve can be drawn according to  $I = g_{GABAE}(V - V_{GABA}) + g_{AMPAE}V + g_{NMDAE}V / (1 + e^{-0.062 * V / 3.57})$ , assuming starting from inhibitory population, the synaptic reversal potentials of excitatory being 0. According to the experiment data of synaptic conductance  $g$  between pyramidal and interneuron population [], with the parameters in TPN:  $g_{GABAE} = 0.0006681, g_{GABAI} = 0.0005120, g_{AMPAE} = 0.0001905, g_{AMPAI} = 0.0001460, g_{NMDAE} = k5 / NI * 0.001, g_{NMDAI} = 60 / NI * 0.001, k5 = [6.15, 7.75, 10.25, 11.25, 12.65, 13.25], NI = 4096$ ; in TNN:  $g_{GABAE} = 0.0006681 * 1.5, g_{GABAI} =$

0.000512\*1.5,  $g_{AMP\Delta E} = 0.0001905*4$ ,  $g_{AMP\Delta I} = 0.0001460*4$ ,  $g_{NMD\Delta E} = 60/NI*0.001$ ,  $g_{NMD\Delta I} = k5/NI*0.001$ ,  $k5 = [6.15,7.75,10.25,11.25,12.65,13.25]$ ,  $NI = 4096$



Quantomechanical, the problem of finding stable state can be discussed on kinematic phase:

In a 3D potential  $V^\beta(\mathbf{x}) = v^\beta(x) + v_\perp(y) + v_\perp(z)$ ,

where  $v$  are single-wells and  $v^a, v^b$  are centered around  $x_0$  and  $0$  individually so that the atom has its state  $|\Psi^+(x)\rangle$  composed by  $\psi^+, \psi_\perp$  (ground-state wave functions of  $v^a$  with eigenvalue  $E_a$  and  $v_\perp$  with eigenvalue  $E_\perp$ ):

$$\langle \mathbf{x} | \Psi^+ \rangle \equiv \Psi^+(\mathbf{x}) = \psi^+(x)\psi_\perp(y)\psi_\perp(z) (***)$$

And  $\Psi^+(x)$  is peaked at the stable point  $x_0 = (x_0, 0, 0)$ , coinciding with the center of  $V^a(x)$  which can be occupied by the  $V^b(x)$ . That is in internal state  $|a\rangle$ , the atom has the motional state which after time  $t$  still unchanged up to its phase  $\varphi^a$  being  $(E_a + 2 E_\perp)t/\hbar$  while in state  $|b\rangle$ , due to the kinematical evolution of  $\varphi^b$ , it will come back to the initial position after oscillating.

If we consider two atoms 1 and 2 both initialized at  $t=0$  with  $|\Psi^+(x)\rangle$  and  $|\Psi^-(x)\rangle$  same as in (\*\*\*) with  $\psi^-(x) \equiv \psi^+(-x)$ . Similar as firing rate model R[I], the particles are subject to step function  $S(x_i)$  related potentials  $\sum_{c=\{+,-\}} S(cx_i) V^{a,b}(cx_i)$ . The reduced form as 1D two particle Schrodinger can be achieved with integrating the variables:

$$\mathcal{H}^{\beta_1, \beta_2} = \sum_{i=1}^2 \left[ \frac{(p_i)^2}{2m} + w^{\beta_i}(x_i, t) \right] + u_x^{\beta_1, \beta_2}(x_1 - x_2)$$

And with setting  $\beta_1 = \beta_2 \equiv \beta$ , the symmetric under particle interchange :

$$|\psi^{\beta\beta}(0)\rangle \approx \frac{|\psi^+\rangle_1 |\psi^-\rangle_2 + |\psi^-\rangle_1 |\psi^+\rangle_2}{\sqrt{2}} \otimes |\beta\rangle_1 \otimes |\beta\rangle_2, \text{ where } \langle \psi^- | \psi^+ \rangle \ll 1 \text{ has been neglected.}$$

This gives out same result that if both atoms are in state  $|a\rangle$ , then due to the collisional phase  $\varphi^{aa} = 0$ , no interaction takes place.

#### 4. CONCLUSION

In general, Hamiltonian markov chain advantage over the markov chain random walk with its faster convergence. As in 2(i) and 2(j), the convergence(variation to mean) of the markov chain hamilton is in blue line and the red line for clinical data and simulation on more possible transition status, giving different convergence but similar phase interval(according to 2(k)), interestingly. The last status transition converge the worst followed by the first transition. And the result simulated with more markov chain status converges better than the clinical results. And according to the convert rate, the mRNA to Protein transfer ratio should be the highest when starting, and goes especially lower in the last two status which is in assistance to the protein binding as we cut off the process around the convergence point where the two population has reached metastability. According to the simulation result, the protein has gone through the switching process changing from normals to persists and back to normal (bursts in optimal time in 2(j) might also due to the switch.).

Mean while, as the second population providing food(protein) to the other's binding site and either activate or deactivate it, it works as the extrinsic noise induced the excitability or exhibition of the other gene. Here, as we choose hax1 and HS 1, they work as promoters for each others. One noticeable computation is the reward computation based on stochastic model selection which is useful in predict the possible status of the cell numbers easily with precomputation. And we can consider correct the transition matrix with simulated clinical tested results to improve the prediction as well. On the other hand, the most important calculation action potential is easier to be achieved through Hamilton as we proved with geometric minimum action and stochastic approximation. Other methods can cover Hamilton Jacobian matrix, WKB and etc. As we also improve the algorithm with adding hierarchical markov in calculating number of cells in different status only record successful move according to the tolerance based on action potential and residual of prediction numbers both, the convergence of the algorithm is guaranteed. And further research can be conducted on the whole process from bifurcation to catastrophe and extinction as well. Problem with multi population is also possible. As hax1 is observed to have function in signaling and regulating of genes especially in learning systems and motor related brain function, this switching model study related to its binding might help to predict the cell numbers and production or degradation rate especially later with further study into both with promoters and persists as to test different drug and their efficiency on the aging process related disease.

In the computation of reachability, the approximation with DTMC mainly compute the kernels of Brownian with shift, finally discretize the original switching diffusion process. As the DTMC gives out the kernel with probability instead of the ratio, it is then convenient to be written into transition matrix  $P_{dx}$  which is discretized from  $S_{dx}$  on finite space state and gives out the reachability with error  $1/h*(K_{dx} + \exp(-2^n - 2^{n/2} + 1))$ .

As the proof in Appendix, the error bounds with Lipschitz constants converged with prominent  $K = mh_1 + Lh_2$ . And the computed result  $N*K*dx$  is here is 0.453 with  $N = 6$ ,  $m = L = 2$ ,  $dx = 0.002$  and  $h_1 = 0.001$ , and  $h_2 = \text{ceil}(h_2*N) = 1.71$ .

Since the final result of the continuous process is not of probability range thus we normalize it with  $P = \text{ratio}/\text{sum}(\text{ratio})$  and the DTMC approximation shown in the figure is the approachability(1-safety.) The result of the test tested continuous embedded matrix and  $h = 0$ ,  $p = 0.0515$ ,  $ci = -0.7212$ ,  $0.0029$ ,  $\text{stats} = \text{struct}$  with  $\text{stat} = -2.2103$  (df: 10), do not reject the hypothesis that the two process. As the final safety consistently for two methods gives highest concentration for the last state showing the example computation's direction from off to on, although there is the slight difference that the forth in the continuous process is relative lower comparing to its other five states as well as the one in the discrete process states. The DTMC

gives strictly increasing concentration from off to on during the 6 states. switching diffusion is a commonly used model in genetic field, not only useful in the transmission of different molecules but also can be derived into analytical models giving straight transfer information about some process with either concentration change or energy change.

About the neuron switch model, it is clear that there is similarity between classical computation and quantum computation with regards to the phase and excitation. This is not surprising since the process identify the excitation is to compare the spectrum with threshold which basically counting on the transform from time domain to frequency domain and such a process can be usually realized with operation on exponent computation while the quantum mechanics is origin from the computation of quantized energy which is also with exponent bases, for instance the most well known poisson distribution and normal distribution as well as the transform as FFT, the same level of computation at the first place correlate these two. And with our experiment, the transform can be illustrated with phase initialized at specific state clearly, thus the entanglement is expressed in quantum computation as well as the classical computation in stability analysis.

As mentioned in the introduction, the similarity exists in the stimulus at hippocampus so as to simulate spontaneous neuron activities and conducting pi-pulse on atoms with different orders so as to excite it to higher states, this is still not quantitatively studied in this paper although some related phase operations are covered, as of both theoretical and experimental value, worth being explored more in the future. Many properties of quantum computation with regards to semantics is also of large usage and since neural network is applied frequently in this field, similar application on quantum computation is also a future direction.

#### ACKNOWLEDGEMENTS

Although I have graduated with excellence graduates awards, I am still working in the university currently cooperated with university neural dynamic lab. Thanks to all the supervisors and colleagues I have worked with.

#### REFERENCES

- [1] Freedman,H.I.,Dynamics of simple gene-network motifs subject to extrinsic fluctua-tions,1980
- [2] Noufe H. Aljahdaly,Analytical Solutions of a Modified Predator-Prey Model through a New Ecological Interaction,2019 ensembl,https://www.ensembl.org/index.html
- [3] Ingo Lohmar, Baruch Meerson, Switching between phenotypes and population extinction, Racah Institute of Physics, 2018
- [4] Daniel Durstewitz1, Jeremy K. Seamans1 and Terrence JRu. Sejnowski1,2, Neurocomputational models of working memory, 2000
- [5] MARCELO CAMPERI, XIAO-JING WANG, A Model of Visuospatial Working Memory in Prefrontal Cortex: Recurrent Network and Cellular Bistability, 1998
- [6] Marta Kwiatkowska, Gethin Norman, David Parker, Stochastic Model Checking, Oxford, 2019
- [7] David Martínez-Rubio, Varun Kanade, Patrick Rebeschini, Decentralized Cooperative Stochastic Bandits, Oxford, 2005 Paul C Bressloff, Stochastic swiching in biology: from genotype to phenotype, Department of Mathematics, University of Utah, 2017 Baier, Christel, Principles of Model checking, Massachusetts Institute of Technology,2008
- [8] Zhu Z, Wang R and Zhu F (2018) The Energy Coding of a Structural Neural Network Based on the Hodgkin–Huxley Model. *Front. Neurosci.* 12:122. doi: 10.3389/fnins.2018.00122
- [9] David Colliaux, Colin Molter, Yoko Yamaguchi, Working memory dynamics and spontaneous activity in a flip-flop oscillations network model with a Milnor attractor, 2009
- [10] D. Jaksch, J.I. Cirac, and P. Zoller, S.L. Rolston, R. Cote and M.D. Lukin , Fast quantum gates for neutral atoms, 2000, **arXiv:quant-ph/0004038v2** , DOI:10.1103/PhysRevLett.85.2208
- [11] Samson Abramsky, Lucien Hardy, Logical Bell Inequalities,2012, arXiv:1203.1352v4

- [12] Cheng Lv, Xiaoguang Li, Fangting Li, Tiejun Li, Constructing the Energy Landscape for Genetic Switching System Driven by Intrinsic Noise, Peking University, 2014
- [13] C.W. Gardiner, Handbook of Stochastic Methods for Physics, Chemistry and the Natural Sciences, 4th ed., Handbook of Stochastic Methods for Physics, Chemistry and the Natural Sciences, 4th ed., Springer, 2009 Alberto Finzi, Thomas Lukasiewicz, Game-Theoretic Agent Programming in GologLuca Cardelli, Marta Kwiatkowska, Robustness Guarantee.Yasar Demirel, in Non-equilibrium Thermodynamics (Third Edition), 2014
- [14] Matthias Heymann, Eric Vanden-Eijnden, Geometric Minimum Action Method: A Least Action Principle on the Space of Curves, Courant Institute, 2007
- [15] Approximate Model Checking of Stochastic Hybrid Systems: Alessandro Abate, Joost-Pieter Katoen, John Lygeros, Maria Prandini. Marta Kwiatkowska, Gethin Norman, Stochastics Model Checking
- [16] Author Robert Balson Dingle, Their Derivation and Interpretation, Academic Press, 1973 J.C., Gittins, Keble College, Oxford, 2010
- [17] Samson Abramsky<sup>1</sup>, Rui Soares Barbosa<sup>1</sup>, Giovanni Carù<sup>1</sup> and Simon Perdrix, A complete characterization of all-versus-nothing arguments for stabilizer states, 2017, <http://dx.doi.org/10.1098/rsta.2016.0385>
- [18] Zahid Ur Rehman, Quorum-Quenching Bacteria Isolated From Red Sea Sediments Reduce Biofilm Formation, KAUST, 2016
- [19] An experimental investigation on the health monitoring of concrete structures using piezoelectric transducers at various environmental temperatures.
- [20] Ali, Isra, Alfarouk, Khalid O., Reshkin, Stephan J., Ibrahim, Muntaser E., Doxycy-cline as Potential Anti-cancer Agent, Anti Cancer Agents, 2018
- [21] Xianjun Cheng, Yue Yuan, Yihong Wang, Rubin Wang, Neural antagonistic mechanism between default-mode and task-positive networks, 2020, DOI: <https://doi.org/10.1016/j.neucom.2020.07.079>
- [22] G.S. Skone, Irina Voiculescu, Stratagems for effective function evaluation in computational chemistry, Oxford, 2010
- [23] Peter Minary, Charlotte M Deane, Exploring peptide/MHC detachment process using hierarchical natural move Monte Carlo, Oxford, 2015 Biancalani, E. Giamperi, A. Bazzani, G. Catellani, and A. Maritan, Phys.Soc, Jpn., Physics, 2015
- [24] D.M. Roma, R.A. P'Flanagan, A.E. Ruckenstein, A.M. Sengupta, R., Optimal path to epigenetic switching, Rarah Institute of Physics, 2015 C HASTE : incorporating a novel multi-scale spatial and temporal algorithm into a large-scale open source library B Y M IGUEL O. B ERNABEU 1, R AFEL B ORDAS 1, P RAS P ATHMANATHAN 1, J OE P ITT -F RANCIS 1, J ONATHAN C OOPER 1, A LAN G ARNY 2, D AVIDJ. G AVAGHAN 1, B LANCA R ODRIGUEZ 1, J AMES A. S OUTHERN AND J ONATHAN P. W HITELEY
- [25] Chris Holmes Leonhard Held Bayesian Auxiliary Variable Models for Binary and Multinomial Regression
- [26] Michael Betancourt and Mark Girolami Hamiltonian Monte Carlo for Hierarchical Model
- [27] rffany Amariuta, Ynag luo, Steven Gazal, Emma E. Davenport, Bryce van de Geijn, Kazuyoshi Ishigaki, Alkes L. Price, IMPACT: Genomic Annotation of Cell-State-Specific Regulatory Elements Inferred from the Epigenome of Bound Transcription Factors.
- [28] Dynamics statistic Markov chain, Alessandro Abate, Joost-Pieter Katoen, Alexandru Mereacrem

## AUTHORS

**Qin He**, Received master degree in data engineering and machine learning with physics minor. During Bachelor (Maths bachelor in ECUST, student union technology and entrepreneur department academic division leader, minor in English), did research study in dynamics neuron networks lab, using statistics, data mining basic skills. Minor in English. In currently master program, doing neuroscience research study related to neuro imaging, neuron computation, minoring in Physics.) Main field in Mathematics and programming, with equal interest in other natural science and technology. And due to past background in machine learning with disciplinary projects, especially related to biomedical and neuroscience in processing time series, frequency spectrums and Bayes models combining stochastic process, computational modeling with python, matlab, C/C++ and a little bit C#.



**Rubin Wang**, Received the Ph.D. degree in electronic and mechanical engineering from Nagoya University, Nagoya, Japan, in 1998., He is currently one of the Director of the Institute of Cognitive Neurodynamics, East China University of Science and Technology, Shanghai, China. His research interests are in the areas of cognitive neurodynamics, coding and decoding theory in brain information processing, complexity theory, analysis of biological neural networks, and computational vision and audition., Dr. Wang serves as the founding Editor-in-Chief of Cognitive Neurodynamics.



**Xiaochuan Pan**, Received the Ph.D. degree in biophysics, University of Chinese Academy of Sciences, in 1997.,He is currently one of the Director of the Institute of Cognitive Neurodynamics, East China University of Science and Technology, Shanghai, China. His research interests are in the areas of cognitive neurodynamics, coding and decoding theory in brain information processing, complexity theory, analysis of biological neural networks, and computational vision and audition. Dt.Pan is professional at behaviour models related to deduction, conditional random dynamics and optimization.



## APPENDIX

Because of paper limit see:

[https://github.com/LilyHeAsamiko/QC/blob/master/UAE\\_ADCCO\(2021.02.21\\_02.17\)/appendix%20of%20Genetic%20Switches%20between%20two%20population%20with%20regards%20to%20mRNA%20and%20proteins%20applying%20Markov%20Chain%20Stochastic%20Model%20Check\\_cor.docx](https://github.com/LilyHeAsamiko/QC/blob/master/UAE_ADCCO(2021.02.21_02.17)/appendix%20of%20Genetic%20Switches%20between%20two%20population%20with%20regards%20to%20mRNA%20and%20proteins%20applying%20Markov%20Chain%20Stochastic%20Model%20Check_cor.docx)